

Gustiness as predictor for lifting sea-salt and dust aerosols in the ECMWF IFS

J.-J. Morcrette^a, A. Beljaars^a, A.
Benedetti^a, L. Jones^a, and O. Boucher^b

^aEuropean Centre for Medium-Range Weather Forecasts, Reading, UK

^bMet Office, Exeter, UK

Research Department

to be submitted to Geophys. Res. Lett.

October 2008

This paper has not been published and should be regarded as an Internal Report from ECMWF.

Permission to quote from it should be obtained from the ECMWF.



European Centre for Medium-Range Weather Forecasts
Europäisches Zentrum für mittelfristige Wettervorhersage
Centre européen pour les prévisions météorologiques à moyen terme

Series: ECMWF Technical Memoranda

A full list of ECMWF Publications can be found on our web site under:

<http://www.ecmwf.int/publications/>

Contact: library@ecmwf.int

©Copyright 2008

European Centre for Medium-Range Weather Forecasts
Shinfield Park, Reading, RG2 9AX, England

Literary and scientific copyrights belong to ECMWF and are reserved in all countries. This publication is not to be reprinted or translated in whole or in part without the written permission of the Director. Appropriate non-commercial use will normally be granted under the condition that reference is made to ECMWF.

The information within this publication is given in good faith and considered to be true, but ECMWF accepts no liability for error, omission and for loss or damage arising from its use.

J.-J. Morcrette^{a1}, A. Beljaars^a, A. Benedetti^a, L. Jones^a, and O. Boucher^b

^aECMWF, Shinfield Park, Reading, RG2 9AX, United Kingdom

^bMetOffice, Fitzroy Road, Exeter, EX1 3PB, United Kingdom

Abstract

The ECMWF IFS model has recently been modified to include prognostic aerosols in its analysis and forecast modules. For the sea salt and dust components, comparisons of three versions of the model are presented: (i) a forecast only model started from conventional analysis with free-running aerosols, (ii) a full analysis including aerosols, and (iii) as in (i) but with sea salt and dust sources revised to account for the 10-m wind including gustiness and calibrated on the aerosol analysis results. It is shown that this new formulation of the sources of the main natural aerosols gives an improved agreement with AERONET surface observations where sea salt and dust aerosols are dominant. It also shows how the information brought by the aerosol analysis could be used to improve the representation of aerosols in numerical weather prediction and climate-type general circulation models.

1 Introduction

As part of the EU-funded GEMS project (Global Environmental Monitoring using Satellite and in situ observations), a 4D-Var reanalysis for the years 2003-2007 is currently being run to estimate atmospheric greenhouse gases, reactive gases and aerosols using satellite-based observations. A prognostic representation of aerosols was developed in the ECMWF (European Centre for Medium-range Weather Forecasts) Integrated Forecast System (IFS) in both its analysis and forecast modules (Morcrette et al., 2007; Benedetti et al., 2008) accounting for sea salt, dust, organic and black carbon, and sulphate aerosols. Sources of sea-salt and dust are interactive with surface and near-surface variables of the model. Other aerosol sources are taken from monthly-mean climatologies (Emission Database for Global Atmospheric Research, Speciated Particulate Emission Wizard) or eight-day mean inventories (Global Fire Emission Database). All aerosols undergo advection, sedimentation, and dry and wet deposition (this last one by large-scale and convective precipitation). For organic matter and black carbon, two components, hydrophobic and hydrophilic, are considered. SO₂ and SO₄ are considered with no explicit chemistry included. Recent developments in the IFS dynamics and package of physical parameterizations allow the aerosols to be advected, and the vertical diffusion and the mass-flux convection schemes to account explicitly for tracers such as aerosols. The wet and dry deposition schemes are standard, whereas the sedimentation of aerosols follows closely the scheme introduced in the IFS for the sedimentation of ice particles.

Recently, the importance of accounting for gustiness in the surface wind used for diagnosing the surface flux of particles was stressed by Glantz et al. (2006), Engelstaedter and Washington (2007), Kurosaki et al. (2007) and Menut (2008). In the following, we present results for sea salt (SS) and dust (DU) for three configurations of the IFS: (1) SS and DU derived from a series of free-running aerosol forecasts (referred to as *FRO*) with the model using 10-m wind (*10W*) as predictor for the emissions; (2) SS and DU resulting from a full meteorological analysis including the 4-D variational assimilation of MODIS aerosol observations with the trajectory computations using the same forecast model are presented (hereafter referred to as *AN*); (3) SS and DU derived from another series of free-running aerosol forecasts (hereafter referred to as *FRA*) in which the analysis results are used to calibrate a new representation of the sources of sea salt and dust based on the 10-m wind including

¹Corresponding author: Jean-Jacques Morcrette, email: Morcrette@ecmwf.int

gustiness (10WIG). Conclusions on the usefulness of such aerosol analysis to improve the representation of aerosols in general circulation models are then drawn.

2 Model

In this study, the ECMWF IFS model is used with a resolution of $T_L159L60$ (i.e., a horizontal grid of $[1.125 \text{ deg}]^2$ and 60 vertical levels from surface to 0.1 hPa). The model is run in either free-running aerosols mode or analysis mode.

In the former mode (without previous aerosol analysis), the model is run with all specific aerosol parametrisations (dry deposition, sedimentation, wet deposition by large-scale and convective precipitation), from 1 December 2002 to 31 January 2005, in a series of 12-hour forecasts starting every 12 hours from the ECMWF operational analyses. The aerosols are started from null concentrations on 1 December 2002 at 00UTC, get produced from surface emission fluxes, and are free-running after that (i.e., the aerosols at the end of a given 12-hour forecast are passed as initial conditions at the start of the next 12-hour forecast). This is in essence not very different from what is done within a transport model, except for the fact that the aerosols go through the dynamics and all other physical parametrisations (vertical diffusion, vertical diffusion and convection) in a consistent manner with the rest of the model.

The analysis is performed on the total aerosol mixing ratio, calculated as the sum of all species (Benedetti et al., 2008). The background fractional contributions (provided by the forward model run as discussed above, from subsequent analyses) are then used to re-distribute the analysis increments of total mixing ratio into the single species. This is achieved through an aerosol mass adjustment using observations of total optical depth derived from the Moderate Resolution Imaging Spectroradiometer (MODIS) instrument on-board of NASA Terra and Aqua satellites. The aerosol observations are ingested through the operational pathway and ingested in the 4D-Var system where they are processed with an ad hoc observation operator specifically designed for aerosol optical depth. This operator uses pre-computed values of optical properties, specific to the different aerosol species at the wavelengths of interest (subsequent results are only presented for 550 nm), in combination with the first-guess values of the aerosol mixing ratios from the model to calculate a profile of extinction. This extinction profile is then vertically integrated to obtain the total aerosol optical depth.

Sea salt and desert dust are each represented by three bins, whose limits are chosen as to have roughly 10, 20 and 70 percent of the mass of each aerosol type in the various bins. The surface flux of sea salt aerosols is parameterized from the 10-m wind at the free ocean surface following Monahan et al. (1986). For the production of desert dust, the source follows an approach similar to Ginoux et al. (2001) and depends on the 10-m wind, soil moisture, the UV-visible component of the surface albedo, and the fraction of land covered by vegetation when the surface is snow-free.

Gusts are defined by WMO as wind extremes that are observed after smoothing the fast signal from an anemometer by a three second running average. The reporting practise is such that gusts are reported as extremes over the previous hour, the previous three or six hours. The mean wind is reported as a ten minute average, which is the last ten-minute interval of the hour. The latter should be comparable with the model ten-meter wind, interpreted as an area average because both the time and spatial averaging operator cancel most of the turbulence spectrum. The model wind gusts are parameterized as the sum of the instantaneous 10-m wind speed and a stability dependent turbulent gustiness

$$U_{10gust} = U_{10} + 7.71U_*f(z_i/L) \quad (1)$$

with

$$f(z/L) = \begin{cases} (1 - 0.021z_i/L)^{1/3} & \text{for } L < 0 \\ 1 & \text{otherwise} \end{cases} \quad (2)$$

where U_{10} is the mean wind speed at 10 m (close to the lowest model level wind), $U_* = |\tau_0|/\rho^{1/2}$ is the friction velocity (itself a function of the 10-m wind speed, with $|\tau_0|$ the absolute surface stress and ρ the density), z_i is the boundary layer height and L is the Monin-Obukhov length scale. The coefficient 7.71 is for a gust duration of three seconds. The z_i/L (buoyancy driven) part of the expression is negligible at strong winds, so the key input to the gust is U_* . The friction velocity is computed from the lowest model level wind using the profile functions also used in the vertical diffusion scheme

$$U_* = \frac{F_{NLEV}}{\ln[(z_{NLEV} + z_0)/z_0] - \Psi_m[(z_{NLEV} + z_0)/L] + \Psi_m(z_0/L)} \quad (3)$$

where F_{NLEV} is the wind speed and z_{NLEV} the height of the lowest model level, Ψ_m is the wind profile stability function and z_0 is the surface roughness length. Again, for strong winds, the Ψ_m functions can be neglected. Overall the gusts are proportional to the mean wind at the lowest model level, with the proportionality factor depending on the roughness length. This factor is small for smooth surfaces (weak turbulence) and large for rough surfaces. The gusts are computed every time-step and estimate the maximum wind (3 s average) within a one hour period (which is of the order of the model time-step).

3 Results

For the month of May 2003, Figures 1 and 2 present, over ocean and land respectively, the global distribution of the monthly mean wind at 10 meters (10W) and the corresponding distribution of the wind at 10 meters including the gustiness (10WIG) as discussed above. Figure 1 shows that the gustiness over ocean can add 20 to 25 percent to the amplitude of the wind in areas of strong surface wind (the Southern hemisphere storm track) but more than 50 percent in low wind areas such as off-coast of Liberia, Sierra Leone ($6^\circ N$, $16^\circ W$) and of South Mexico ($16^\circ N$, $100^\circ W$). Similarly Figure 2 shows that, over land, considering gustiness increases the amplitude of the surface wind by more than 50 percent over areas of low wind (Amazonia, Central Africa) and by 25 to 30 percent over North Sahara, South Central USA, South Argentina and all over South West Asia from Pakistan and India to West China. If a source function following Monahan et al. (1986) is used for diagnosing the emission of sea salt, the power 3.41 applied to the surface wind would roughly double the emission when using 10WIG instead of 10W. Therefore, from comparison of the pdf's of 10W and 10WIG and that of the *FRA* and *AN SS*, a globally defined normalization factor around 0.5 has been introduced in the parameterization of the emission of sea salt aerosols when using 10WIG as predictor. For dust production, the IFS makes the production of dust aerosols proportional to the dust emission potential (*DEP*, which is a function of the soil type and soil moisture) and to $(V - LTS)V^2$ where V is either 10W or 10WIG, *LTS* is the lifting threshold speed depending on the mean radius of the particle, soil moisture, the UV-visible component of the surface albedo from MODIS, and the fraction of cover by vegetation when the surface is snow-free. When using 10WIG as predictor, a normalization factor similar to the one for sea salt emission is also used.

Figures 3 and 4 present, averaged over May 2003, for the sea salt and dust component respectively, the optical depth at 550 nm (τ_{550}) from the free-running forecast model, the corresponding quantity from the analysis of MODIS optical depth, and the free-running forecast model with the revised formulation calibrated on the analysis results. The revised formulations clearly allow the free-running model to get in much better agreement with the analysis, both for sea salt and dust aerosols. The improvement in τ_{550}^{SS} for sea salt is obtained simply using 10WIG as discussed above. The improvement is seen over the areas of strong wind (South Hemisphere

storm track) but also in the subtropical areas. For dust, the revised formulation not only uses *10WIG* but also the geographically relevant *DEP*'s adjusted to give the best agreement possible with the analyzed τ_{550}^{DU} for dust. The adjustment clearly improves the distribution of τ_{550}^{DU} from Saudi Arabia to India, and over Northern China. It also makes dust appearing over the South West USA, around the Atacama desert and Australia.

Figures 5 and 6 compare over the month of May 2003 the time-series of τ_{550}^{SS} and τ_{550}^{DU} from *FRO*, *AN* and *FRA*, with the τ_{500} measured for some AERONET stations (Holben et al., 1998) where either sea salt or dust aerosols are prevailing (see Table 1). Those stations were selected based on both the observed Angstrom exponent and the model τ_{550}^{SS} or τ_{550}^{DU} being at least 90 percent of the model total τ_{550} . In Figure 5, for Amsterdam Island and Rottneest Island, *FRA* provides a smaller τ_{550}^{SS} than *FRO*. For Nauru and Tahiti, *FRA* provides a slightly larger τ_{550}^{SS} than *FRO*. For dust (Figure 6), *FRA* is generally in much closer agreement with *AN* than *FRO*, with a general increase of τ_{550}^{DU} over periods when peaks of dust occur. Over the month, whether for sea-salt or dust, in most cases, *FRA* optical depth is closer to *AN* optical depth.

4 Conclusion

In this study, the ECMWF IFS was integrated including a prognostic representation of aerosols. Comparisons were made of τ_{550} for sea salt and dust from 12-hour forecasts with free-running aerosols, from an analysis of meteorological observations including MODIS aerosol optical depth, and from forecasts with an improved representation of the sea salt and dust aerosols using the 10 meter wind including gustiness and revised source parameterizations calibrated on the analysis results. This approach to improving the representation of aerosols is clearly successful and could lead to an improved knowledge of the four-dimensional distribution of various aerosols. This study has concentrated on natural aerosols, whose sources are interactive with the rest of the model. A similar approach could be used to improve the representation of other aerosols, whose sources are still poorly described in inventories and could be improved with the technique discussed in this paper.

Acknowledgments

This report is dedicated to the memory of Tony Hollingsworth whose vision and energy made the GEMS project possible. Observational data for the individual stations in Figures 5 and 6 were obtained from the AERONET web site. Brent Holben and his collaborators are thanked for their efforts in establishing and maintaining the AERONET sites used in this study. The MODIS data used as part of the analysis were downloaded from the NASA Giovanni server.

References

- Benedetti, A., J.-J. Morcrette, O. Boucher, A. Dethof, R.J. Engelen, M. Fisher, H. Flentjes, N. Huneus, L. Jones, J.W. Kaiser, S. Kinne, A. Mangold, M. Razinger, A.J. Simmons, M. Suttie, and the GEMS-Aerosol team, 2008: Aerosol analysis and forecast in the ECMWF Integrated Forecast System. Part II: Data assimilation. *ECMWF Technical Memorandum*, **571**, 25 pp.
- Engelstaedter, S. and R. Washington, 2007: Temporal controls on global dust emissions: The role of surface gustiness. *Geophys. Res. Lett.*, **34**, L15805, doi:10.1029/2007GL029971.
- Ginoux, P., M. Chin, I. Tegen, J. Prospero, B.N. Holben, O. Dubovik, and S.-J. Lin, 2001: Sources and distributions of dust aerosols simulated with the GOCART model. *J. Geophys. Res.*, **106D**, 20255-20274.

Glantz, P., D.E. Nilsson, and W. von Hoyningen-Huene, 2006: Estimating a relationship between aerosol optical thickness and surface wind speed over the ocean. *Atmos. Chem. Phys. Discuss.*, **6**, 11621-11651.

Holben, B.N., T.F. Eck, I. Slutsker, D. Tanre, J.P. Buis, A. Setzer, E. Vermote, J.A. Reagan, Y.J. Kaufman, T. Nakajima, F. Lavenu, I. Jankowiak, A. Smirnov, 1998: An emerging ground-based aerosol climatology: Aerosol optical depth from AERONET. *J. Geophys. Res.*, **106D**, 12067-12097.

Kurosaki, Y. and M. Mikami, 2007: Threshold wind speed for dust emission in east Asia and its seasonal variations. *J. Geophys. Res.*, **112**, D17202, doi: 10.1029 /2006JD007988.

Menut, L., 2008: Sensitivity of hourly Saharan dust emissions to NCEP and ECMWF modeled wind speed. *J. Geophys. Res.*, **113**, D16201, doi: 10.1029 /2007JD009522.

Monahan, E.C., K.L. Davidson and D.E. Spiel, 1986: Whitecap aerosol productivity deduced from simulation tank measurements. *J. Geophys. Res.*, **87**, 8898-8904.

Morcrette, J.-J., O. Boucher, L. Jones, D. Salmond, P. Bechtold, A. Beljaars, A. Benedetti, A. Bonet, J.W. Kaiser, M. Razinger, M. Schulz, S. Serrar, A.J. Simmons, M. Sofiev, M. Suttie, A. Tompkins, A. Untch and the GEMS-AER team, 2008: Aerosol analysis and forecast in the ECMWF Integrated Forecast System: Forward modelling. *ECMWF Technical Memorandum*, **573**, 35 pp.

| Station | Latitude | Longitude | Main aerosol |
|------------------|----------|-----------|--------------|
| Amsterdam Island | 37.81 S | 77.57 E | SS |
| Nauru | 0.52 S | 166.92 E | SS |
| Rottneest Island | 32.00 S | 115.50 E | SS |
| Tahiti | 17.58 S | 149.61 W | SS |
| Blida | 36.51 N | 2.88 E | DU |
| Dahkla | 23.72 N | 15.95 W | DU |
| Dalanzadgad | 43.58 N | 104.42 E | DU |
| Forth Crete | 35.33 N | 25.28 E | DU |
| Sede Boker | 30.86 N | 34.78 E | DU |
| Solar Village | 24.91 N | 46.40 E | DU |

Table 1: The coordinates and dominant aerosol type (SS=sea salt, DU=dust) for the comparison of model optical depth shown in Figures 5 and 6.

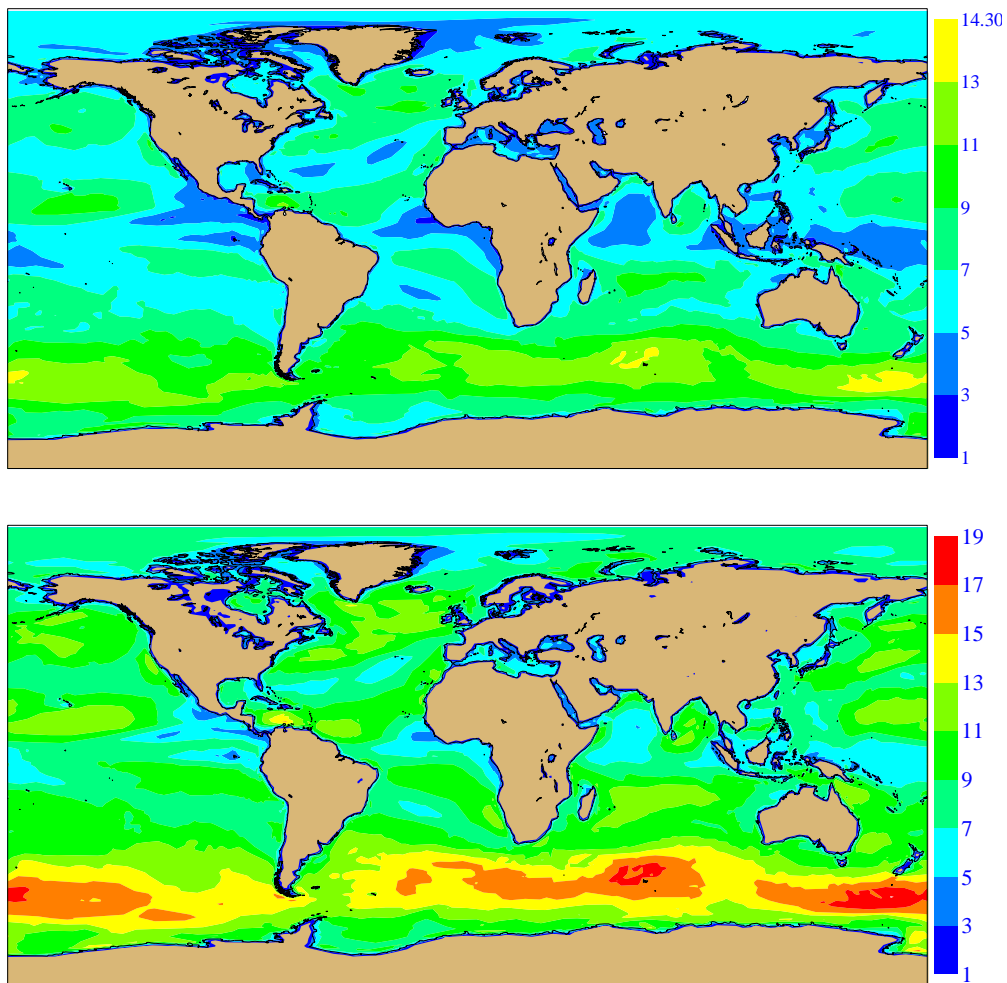


Figure 1: The wind at 10 meters over ocean for May 2003 (in ms^{-1}). Top figure is the usual 10-m wind, bottom figure is the 10-m wind including the gusts (see text).

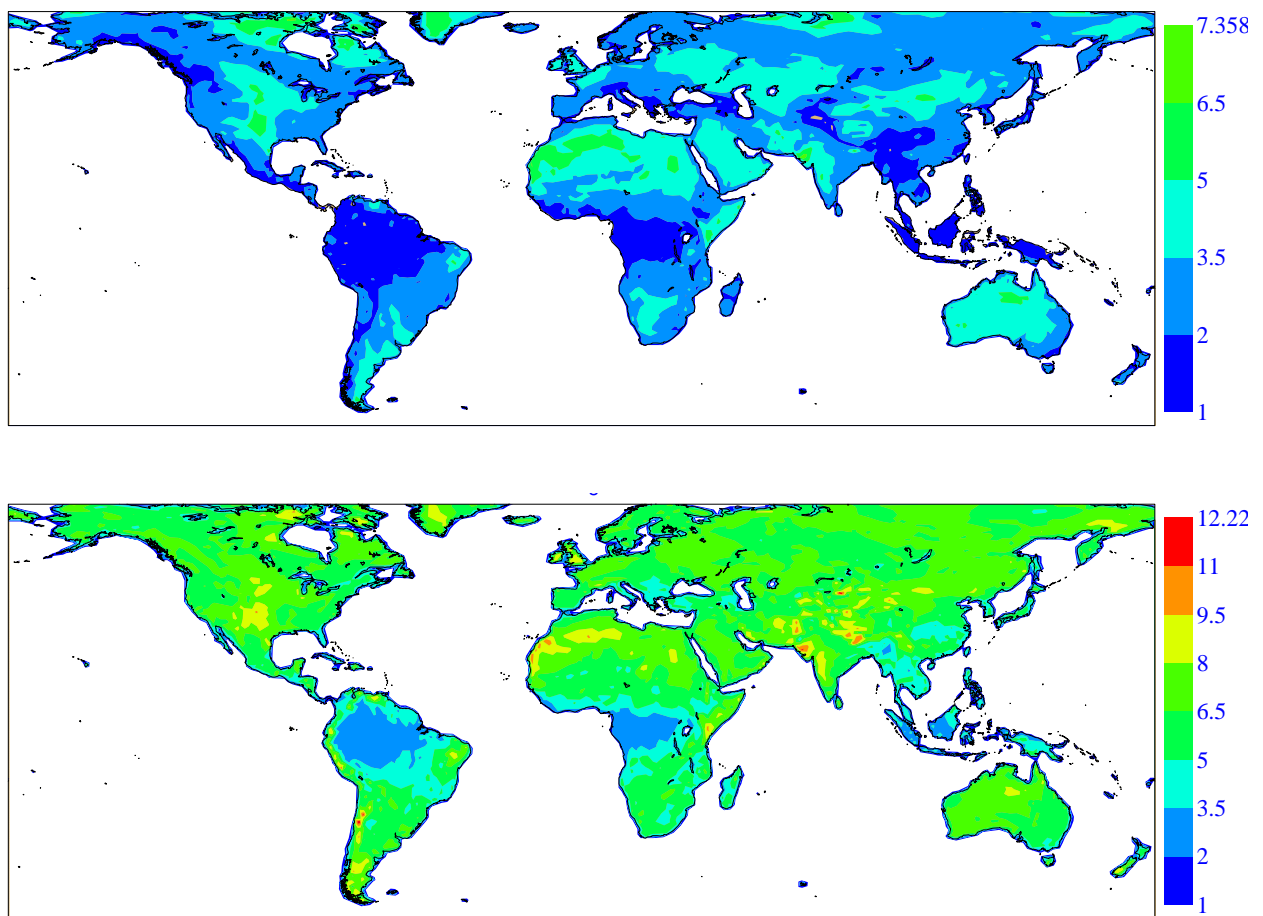


Figure 2: The wind at 10 meters over land for May 2003 (in ms^{-1}). Top figure is the usual 10-m wind, bottom figure is the 10-m wind including the gusts (see text).

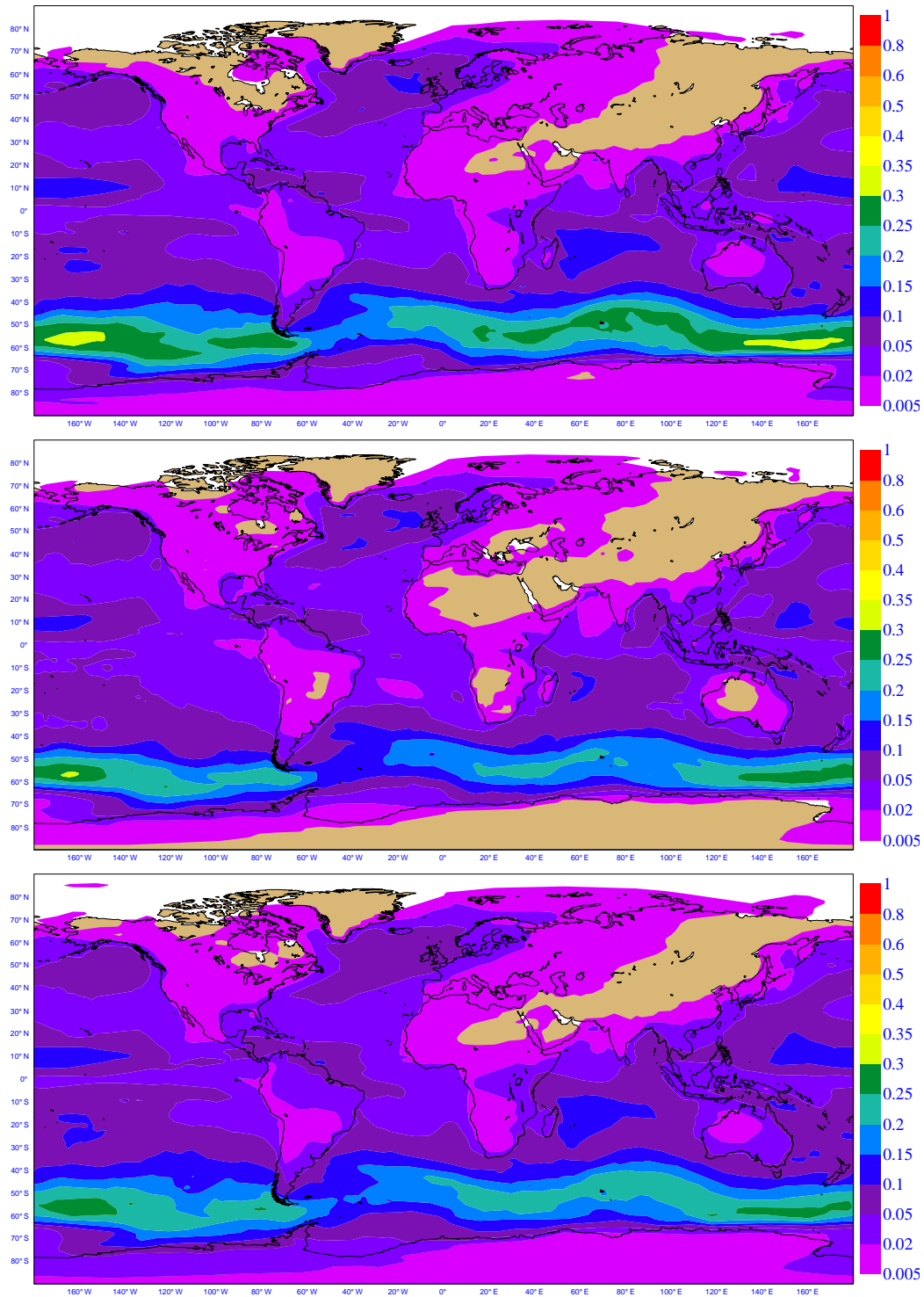


Figure 3: The optical depth at 550 nm of the sea salt component. Top panel is the free-running forecast, middle panel is the analysis, bottom panel is the free-running model revised and calibrated on the analysis results.

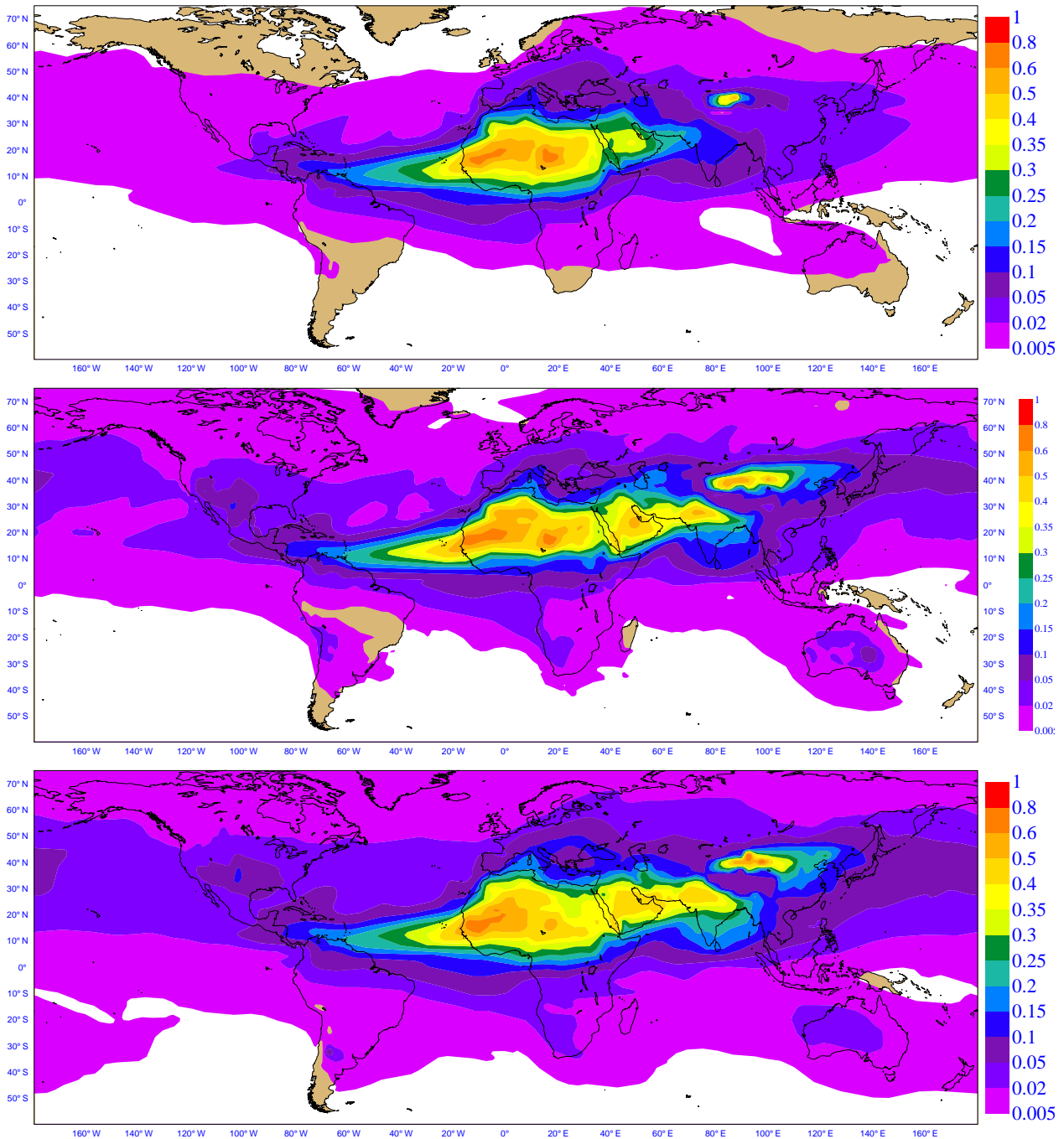


Figure 4: The optical depth at 550 nm of the dust component. Top panel is the free-running forecast, middle panel is the analysis, bottom panel is the free-running model revised and calibrated on the analysis results.

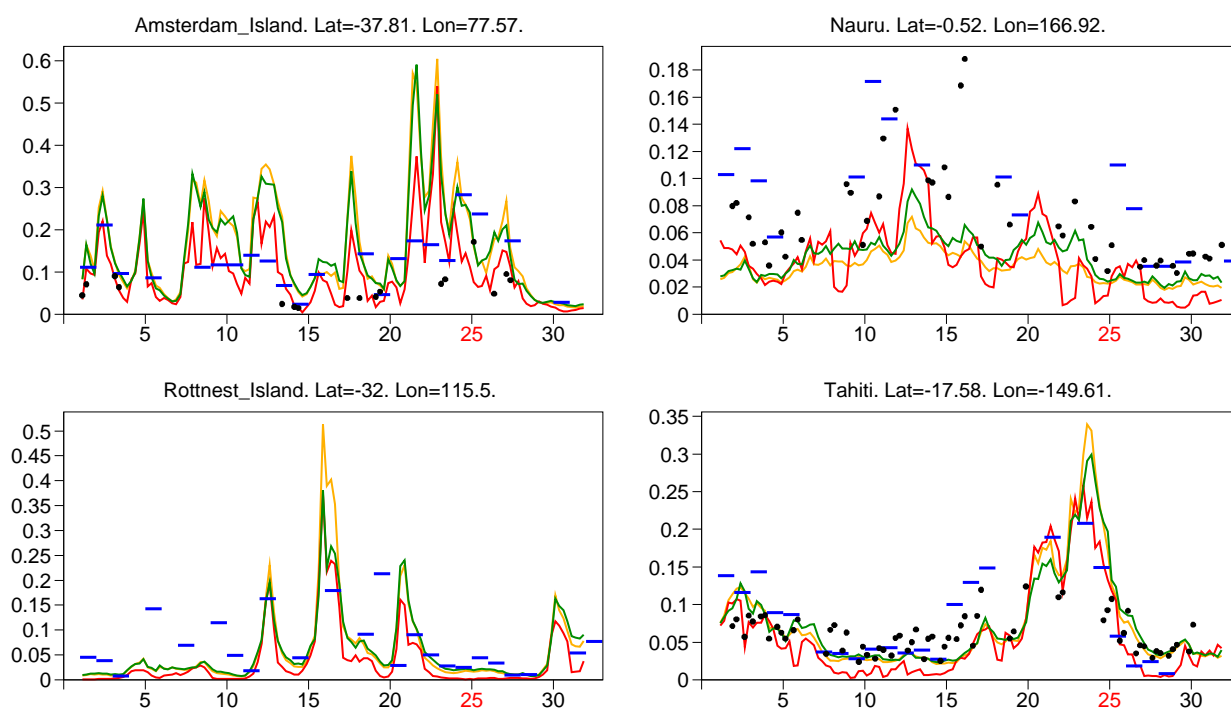


Figure 5: Time-series of the optical depth at 550 nm over the AERONET stations of Amsterdam Island, Nauru, Rottneest Island and Tahiti. Model results for FR0 (yellow), AN (red), FRA (green) are for sea salt only with the AERONET observations of total optical depth (black dots) and the MODIS-derived optical depth (blue segments). See table 1 for the location of the stations.

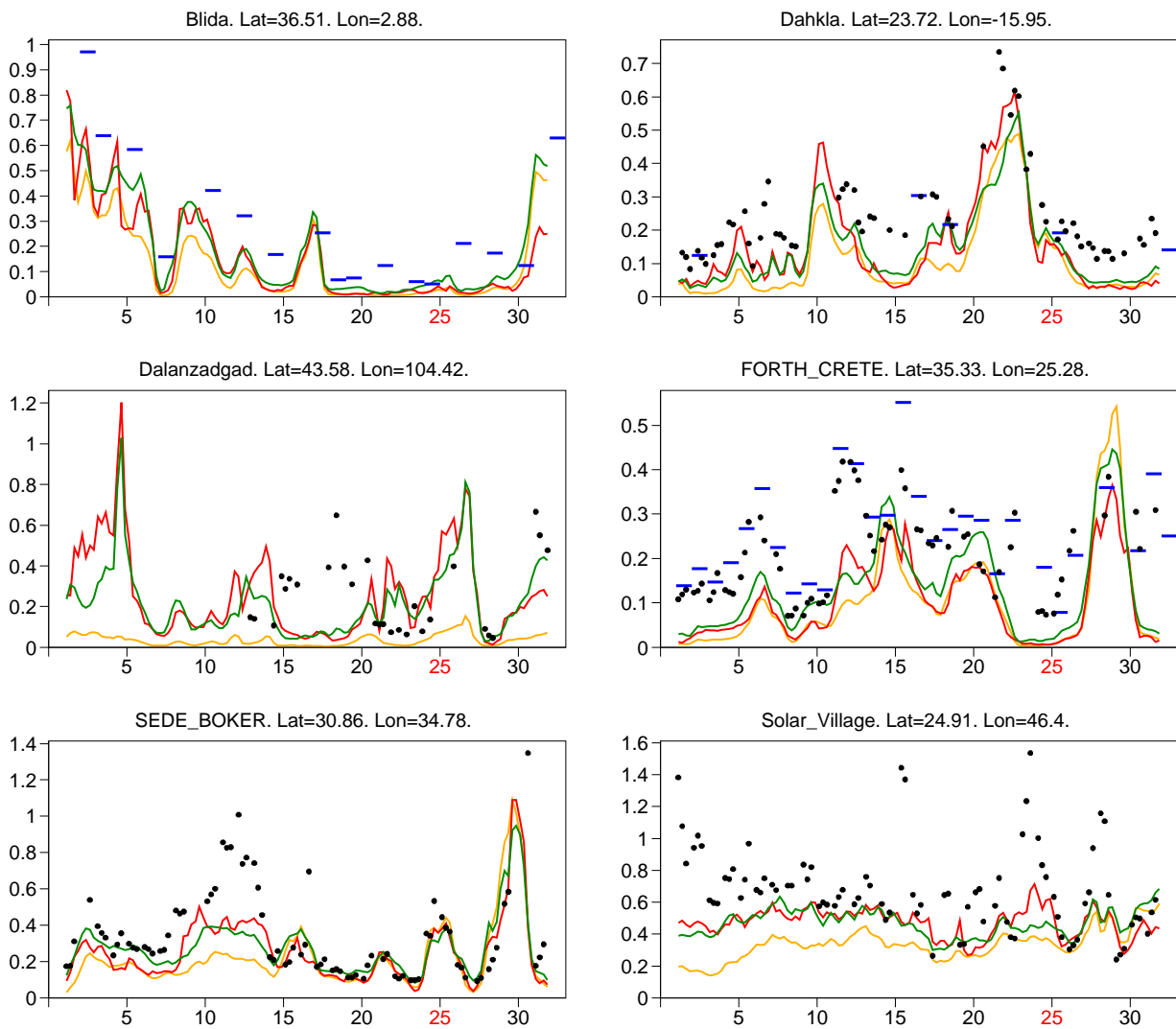


Figure 6: As in Figure 5, but for the time-series of the optical depth at 550 nm over the AERONET stations of Blida, Dahkla, Dalanzadgad, Forth Crete, Sede Boker and Solar Village. Model results for FR0 (yellow), AN (red), FRA (green) are for dust only with the AERONET observations of total optical depth (black dots) and the MODIS-derived optical depth (blue segments). See table 1 for the location of the stations.